



Since January 2020 Elsevier has created a COVID-19 resource centre with free information in English and Mandarin on the novel coronavirus COVID-19. The COVID-19 resource centre is hosted on Elsevier Connect, the company's public news and information website.

Elsevier hereby grants permission to make all its COVID-19-related research that is available on the COVID-19 resource centre - including this research content - immediately available in PubMed Central and other publicly funded repositories, such as the WHO COVID database with rights for unrestricted research re-use and analyses in any form or by any means with acknowledgement of the original source. These permissions are granted for free by Elsevier for as long as the COVID-19 resource centre remains active.



Catalytic hairpin DNA assembly-based chemiluminescent assay for the detection of short SARS-CoV-2 target cDNA

Ji Yoon Do, Ji Yun Jeong, Cheol Am Hong^{*}

Department of Biochemistry, Yeungnam University, 280 Daehak-ro, Gyongsan-si, Gyeongsangbuk-do, 38541, Republic of Korea

ARTICLE INFO

Keywords:

Catalytic hairpin assembly
Chemiluminescent assay
Colorimetric detection
SARS-CoV-2
Target DNA
DNA probe

ABSTRACT

Colorimetric sensors are recognized as a promising means for target molecule detection as they provide rapid, cost-effective, and facile sensing visible to the naked eye. Challenges remain though in terms of their detection sensitivity and specificity for short-length target genes. Herein, we demonstrate the successful combination of the catalytic hairpin DNA assembly (CHA) approach with enzyme-linked immunosorbent assay (ELISA)-mimicking techniques for a simple, sensitive, and sequence-specific colorimetric assay to detect short SARS-CoV-2 target cDNA. In the developed CHA-based chemiluminescent assay, a low concentration of target cDNA is continuously recycled to amplify dimeric DNA probes from two biotinylated hairpin DNA until the hairpin DNA is completely consumed. The dimeric DNA probes are effectively immobilized in a neutravidin-coated microplate well and then capture neutravidin-conjugated horseradish peroxidase via biotin-neutravidin interactions, resulting in a sensitive and selective colorless-to-blue color change. The developed sensing system exhibits a high sensitivity with a detection limit of ~1 nM for target cDNA as well as the ability to precisely distinguish a single-base mismatched mutant gene within 2 h. As the proposed system does not require complex protocols or expensive equipment to amplify target cDNA, it has the potential to be utilized as a powerful tool to improve the detection sensitivity of target genes for clinical diagnostics with colorimetric detection.

1. Introduction

DNA is recognized as a promising biomarker for clinical diagnostics because its specific sequences are closely related to the cause and development of diseases [1–3]. In this field, achieving rapid, reliable, and accurate diagnosis is critical to improve patient care and infection control. Real-time polymerase chain reaction (RT-PCR) is currently among the most widely used diagnostic techniques to detect specific DNA owing to its excellent specificity and sensitivity [4,5]. This system is an enzyme-driven reaction that can exponentially amplify very low amounts of DNA to detectable levels via repeated thermal cycles of heating and cooling. However, RT-PCR systems often rely on experimental procedures that are complex, expensive, labor-intensive, and time-consuming, leading to limitations in point-of-care analysis and rapid diagnosis. In particular, the detection of single nucleotide polymorphisms and short DNA with less than 30 nucleotides remains a significant challenge for accurate diagnosis.

In recent years, increasing attention has been paid to enzyme-free isothermal DNA amplification due to its efficient and rapid detection,

in which short DNA is amplified through toehold-mediated strand displacement (TMSD) reactions [6–8]. A variety of TMSD-based DNA amplification techniques have been developed and are currently utilized in clinical applications, including the catalytic hairpin DNA assembly (CHA) [9,10] and hybridization chain reaction (HCR) [11,12]. These amplification strategies are carried out using hairpin DNA, which spontaneously hybridizes to generate a variety of hairpin complexes (e. g., nanowires, dendrimers, and hydrogels) when single-stranded target DNA is presented [13–16]. During the hybridization process, the target DNA is spontaneously released from the hairpin complex, allowing it to induce more hairpin opening and assembly events. The hairpin complexes combine with detection techniques like fluorescent [17–20], colorimetric [21–23], or electrochemical [24–26] sensors to improve the signal amplification and transduction of the target DNA, thereby enhancing the detection of very low abundance target DNA.

The enzyme-linked immunosorbent assay (ELISA) is the most promising colorimetric sensor because it allows us to reliably distinguish analytes through comparing color changes [27–30]. ELISA sensors detect antibody–antigen interactions to effectively highlight the

^{*} Corresponding author.

E-mail address: cahong@yu.ac.kr (C.A. Hong).

<https://doi.org/10.1016/j.talanta.2021.122505>

Received 24 March 2021; Received in revised form 4 May 2021; Accepted 5 May 2021

Available online 16 May 2021

0039-9140/© 2021 Elsevier B.V. All rights reserved.

presence of specific proteins (e.g., antibody, antigen, or glycoprotein) in biological samples [31–33]. Recently, the development of high-throughput automated ELISA systems has enabled the rapid analysis of large numbers of samples at once, leading to the wide adoption of such systems in clinical applications for detecting viral infections such as from human immunodeficiency virus (HIV), severe acute respiratory syndrome coronavirus 2 (SARS-CoV-2), and influenza virus, due to their rapid, sensitive, and low-cost methods [34,35]. However, these systems have relatively lower sensitivity for accurately detecting viruses lying dormant within a cell.

In this study, we combine CHA with ELISA-mimicking techniques to develop a CHA-based chemiluminescent assay for the simple, sensitive, and specific colorimetric detection of short SARS-CoV-2 target complementary DNA (cDNA). The developed assay employs two types of catalytic hairpin DNA containing a biotin at the 5' ends that continuously produce di-biotinylated dimeric DNA probes through target cDNA-triggered recycling reactions. The resultant dimeric DNA probes are specifically anchored in a neutravidin-coated microplate well, which enables neutravidin–horseradish peroxidase (NA-HRP) to be strongly immobilized on the probes for colorimetric detection. The designed CHA reactions are initiated and recycled only by the target cDNA, thus achieving a high detection sensitivity even with low concentrations of target cDNA presented. Ultimately, the developed CHA-based chemiluminescent assay exhibits both rapid and accurate discrimination of target cDNA as well as single-base mismatched target cDNA mutations.

2. Material and methods

2.1. Oligonucleotides

All DNA oligonucleotides were purchased from Bioneer Inc. (Daejeon, Republic of Korea); their sequences are shown in Table S1.

2.2. Polyacrylamide gel electrophoresis (PAGE) analysis

All DNA products were verified by 12% PAGE in 1X TAE (Trizma base, acetic acid, and 0.5 M EDTA, at pH 8.0) buffer at 150 V for 45 min. The gel was stained with GelRed® (Biotium, USA) for 1 min and visualized using a GelDoc Go system (Bio-Rad, USA).

2.3. Amplification of dimeric DNA probes

Biotinylated DNA oligonucleotides (HD1 and HD2) were completely dissolved in 1X phosphate buffered saline (PBS, at pH 7.4). Each resultant product was heated to 94 °C for 5 min and then rapidly cooled to 10 °C using a thermal cycler (BIOER, China) to form stable hairpin DNA nanostructures. To amplify dimeric DNA probes, target cDNA was added to a mixture of HD1 and HD2 and then incubated for different periods of time at room temperature. The resultant products, dimeric DNA probes, were verified using 12% PAGE analysis. The band intensity was quantitatively compared using GelDoc Go image software (Bio-Rad, USA).

2.4. Chemiluminescent assay

HD1, HD2, and target cDNA were incubated for 60 min at room temperature. The resultant mixture was added to a 96-well plate pre-coated with neutravidin proteins (Thermo Fisher Scientific, USA) at room temperature. After 20 min, the solution was removed and washed three times with a washing buffer, PBS with 1% Tween 20® detergent (PBST). The plate was then incubated with horseradish peroxidase (HRP) conjugated with neutravidin (Thermo Fisher Scientific, USA) solution containing with 1% skim milk for 10 min at room temperature. After washing five times with 1X PBS, 1-Step™ TMB-EILSA substrate solution (Thermo Fisher Scientific, USA) was added to the resultant plate and then incubated for 5 min at room temperature with gentle shaking. The chemiluminescent signals were measured at 650 nm using an Epoch

2 microplate Spectrophotometer (BioTek, USA).

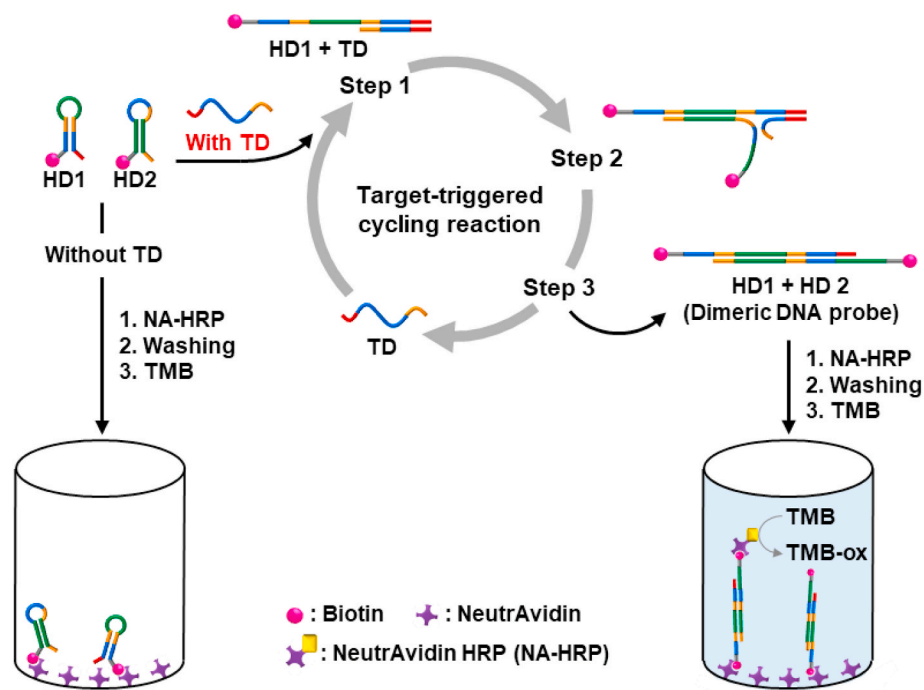
3. Results and discussion

3.1. Principle of the CHA-based chemiluminescent assay

The principle of the designed CHA-based chemiluminescent assay for the colorimetric detection of short SARS-CoV-2 target cDNA is schematically illustrated in Scheme 1. Two individual hairpin DNA (HD), HD1 and HD2, are designed to have structural analogs and complementary base pairing with each other. These HDs consist of two single-stranded toeholds at the 3' end (6 nt) and the 5' end (5 nt), a double-stranded stem (18 bp), and a single-stranded loop (12 nt). Each 5' end of the two HDs is labeled with a biotin molecule. In the presence of target cDNA (TD), the short toehold at the 3' end of HD1 hybridizes with the TD and opens its stem, resulting in the formation of HD1+TD intermediates having newly exposed sticky ends (Step 1 in Scheme 1). These exposed sticky ends (35 nt) can self-assemble with the 3' end toehold of HD2, which simultaneously releases the hybridized TD because of competitive hybridization (Step 2 in Scheme 1), resulting in the formation of dimeric DNA probes containing a biotin at each 5' end (Step 3 in Scheme 1). Notably, the released TD can interact repeatedly with HD1 to generate a large amount of dimeric DNA probes without any enzymatic or chemical reactions through the designed TD-triggered recycling reactions. The biotin-labeled dimeric DNA probes are able to be effectively anchored to the bottom of neutravidin-coated microplate wells via biotin–neutravidin interactions [36], which also serve as a capture probe to immobilize the neutravidin-labeled HRP in the well. After the addition of TMB solution, the HRP loaded in the well catalyzes the oxidation of the colorless TMB into blue TMB⁺. Note that in the absence of TD, the TD-triggered recycling reactions do not trigger the amplification of dimeric DNA probes, resulting in no color development in the well. Thus, the proposed CHA-based chemiluminescent assay has the potential to be used to detect specific target genes by visual observation.

3.2. Feasibility of TD-triggered recycling reactions

To verify the feasibility of the TD-triggered recycling reactions in the catalytic hairpin DNA, the formation of dimeric DNA probes was confirmed through polyacrylamide gel electrophoresis (PAGE) analysis. For SARS-CoV-2 detection, we employed two different target genes, *N* and *E* cDNA, known as novel markers to detect SARS-CoV-2 RNA genes [37,38]. As shown in Fig. 1A, the *N* gene targeted HDs, *N*-HD1 and *N*-HD2 (line 2 and line 3), showed only one bright single band, indicating the successful formation of monodispersed hairpin DNA nanostructures without non-specific aggregation. Upon the mixing of *N*-HD1 and the *N* gene target cDNA (*N*-TD), we observed a notable band shift related to *N*-HD1+*N*-TD intermediated products (line 4 in Fig. 1A) as compared to its composites. Notably, in the presence of *N*-TD in a mixture of *N*-HD1 and *N*-HD2, the band corresponding to *N*-HD1 and *N*-HD2 disappeared, while a new band appeared (line 6 in Fig. 1) that migrated more slowly than the *N*-HD1+*N*-TD products, thus demonstrating the successful formation of dimeric DNA probes, *N*-HD1+*N*-HD2 products, through the proposed target cDNA-triggered recycling reactions. The synthetic yields of the dimeric DNA probes were approximately 90% as measured by densitometry. However, in the absence of *N*-TD in a mixture of *N*-HD1 and *N*-HD2, no significant band shift appeared under the same conditions (line 7 in Fig. 1A). This result indicates that the TD plays an important role as the initiator to trigger the formation of the dimeric DNA probes through the TD-triggered recycling reactions. In addition, the same gel results were observed in the designed *E* gene target cDNA (*E*-TD)-triggered recycling reactions (Figure S1A), indicating that the developed TD-triggered recycling reactions can potentially be utilized as a promising platform to detect several types of target sequences.



Scheme 1. Schematic illustration of the catalytic hairpin DNA assembly (CHA)-based chemiluminescent assay for sequence-specific and colorimetric detection of target genes. HD is hairpin DNA; TD is target DNA.

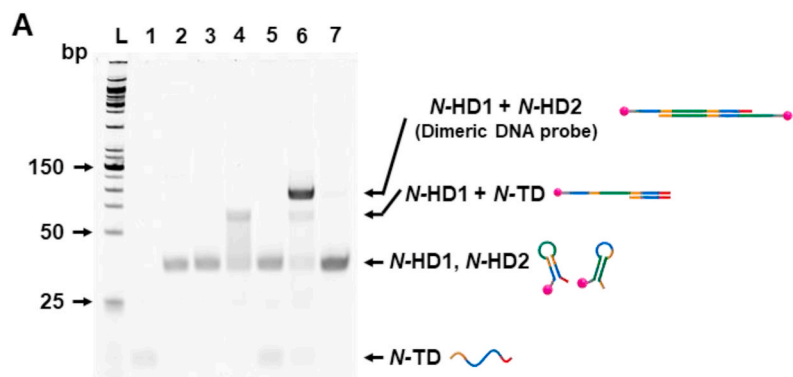
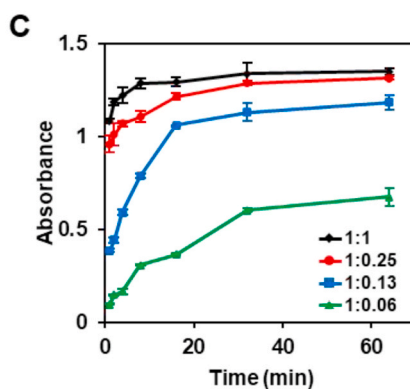
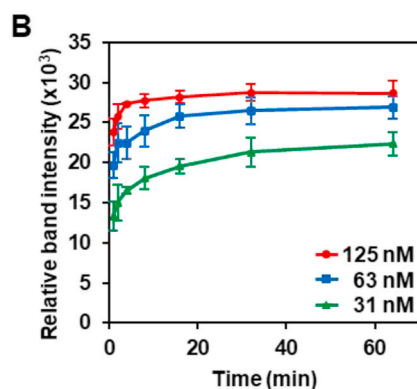


Fig. 1. (A) 12% PAGE analysis to confirm the formation of dimeric DNA probes in the presence of *N* gene target cDNA (*N*-TD). Lane L: DNA ladder; Lane 2: *N*-HD1; Lane 3: *N*-HD2; Lane 4: *N*-HD1+*N*-TD; Lane 5: *N*-HD2+*N*-TD; Lane 6: *N*-HD1+*N*-HD2+*N*-TD; Lane 7: *N*-HD1+*N*-HD2. (B) Time-dependent profile of the gel band intensity of dimeric DNA probes upon mixing 500 nM HD with various concentrations of *N*-TD. (C) Time-dependent profile of the chemiluminescent signals from the CHA-based chemiluminescent assay at various molar ratios of HD to TD. Error bars show the standard deviation of three independent experiments.



In order to confirm whether the TD is indeed recycled in amplifying the dimeric DNA probes, we investigated the amount of dimeric DNA probes generated from the HD (500 nM) over time at various concentrations of TD: 31, 63, and 125 nM. As shown in Fig. 1B, with increasing

TD concentration and incubation time, the amount of synthesized dimeric DNA probes gradually increased and reached a plateau. Saturation of the synthesized dimeric DNA probes was observed around 4 min when using 125 nM TD and around 16 min when using 63 nM TD,

while no plateau was reached at the relatively low TD concentration of 31 nM over a period of 64 min. We also examined the cycling efficiency of TD in generating dimeric DNA probes from a mixture of 500 nM HDs and 125 nM TD over time (Figure S2). With increasing incubation time, the amount of synthesized dimeric DNA probes gradually increased and reached a plateau. Notably, at a relatively low incubation time ranging from 1 min to 6 min, a linear relationship between the dimeric DNA probes and incubation time was observed. Based on the resultant correlations, approximately 15 nM of the dimeric DNA probes per minute was generated via the proposed target-triggered cycling reaction. These results strongly suggest that the TD acts as both initiator and catalyst for amplifying the dimeric DNA probes in the recycling reactions. Thus, even at low concentrations of TD, dimeric DNA probes are able to be sufficiently amplified until the HD is completely consumed by the recycling reactions.

We further investigated the effect of the TD-triggered recycling reactions on the detection sensitivity of the chemiluminescent signals for the target genes (Fig. 1C). Upon mixing HD and TD at a 1:1 molar ratio, the chemiluminescent signals gradually increased and reached a plateau at 8 min because of the complete consumption of the HDs in forming dimeric DNA probes, representing a rapid saturation as compared to that with relatively lower HD:TD molar ratios, namely 1:0.6, 1:0.25, and 1:0.13. This result suggests that the chemiluminescent signal efficiency depends on the amount of dimeric DNA probes formed in the target DNA-triggered recycling reactions. With sufficient time for the TD-

triggered recycling reactions, the dimeric DNA probes can be effectively amplified even in the presence of low-concentration TD, resulting in an improved detection sensitivity of the chemiluminescent signals.

3.3. Optimization of the experimental conditions

To obtain the best assay performance, several experimental conditions such as incubation time and the concentrations of HDs and neutravidin-HRP (NA-HRP) were explored. We first optimized the concentrations of the HDs to obtain the highest detection sensitivity for target genes by adding various concentrations of dimeric DNA probes into neutravidin-coated microplate wells. The dimeric DNA probes were prepared by mixing TD and HDs at a 1:1 molar ratio for 20 min. As shown in Fig. 2A, the chemiluminescent signals were distinctly detected at an HD concentration of 300 nM, gradually increased until peaking at 500 nM, and then gradually decreased from 1000 nM to 1500 nM. Accordingly, we chose 500 nM as the optimized concentration to amplify the dimeric DNA probes. Next, we explored the optimized concentration of NA-HRP (Fig. 2B). Serial dilutions of NA-HRP (1/1000, 1/5000, 1/10000, 1/50000, and 1/100000) were used to investigate the corresponding color changes in the microplate wells in the presence and absence of TD. At 1/1000 dilution, non-specific color change was observed in the absence of TD due to the non-specific binding of NA-HRP onto the microplate well, while relatively higher dilution factors did not show such non-specific color change under the same conditions.

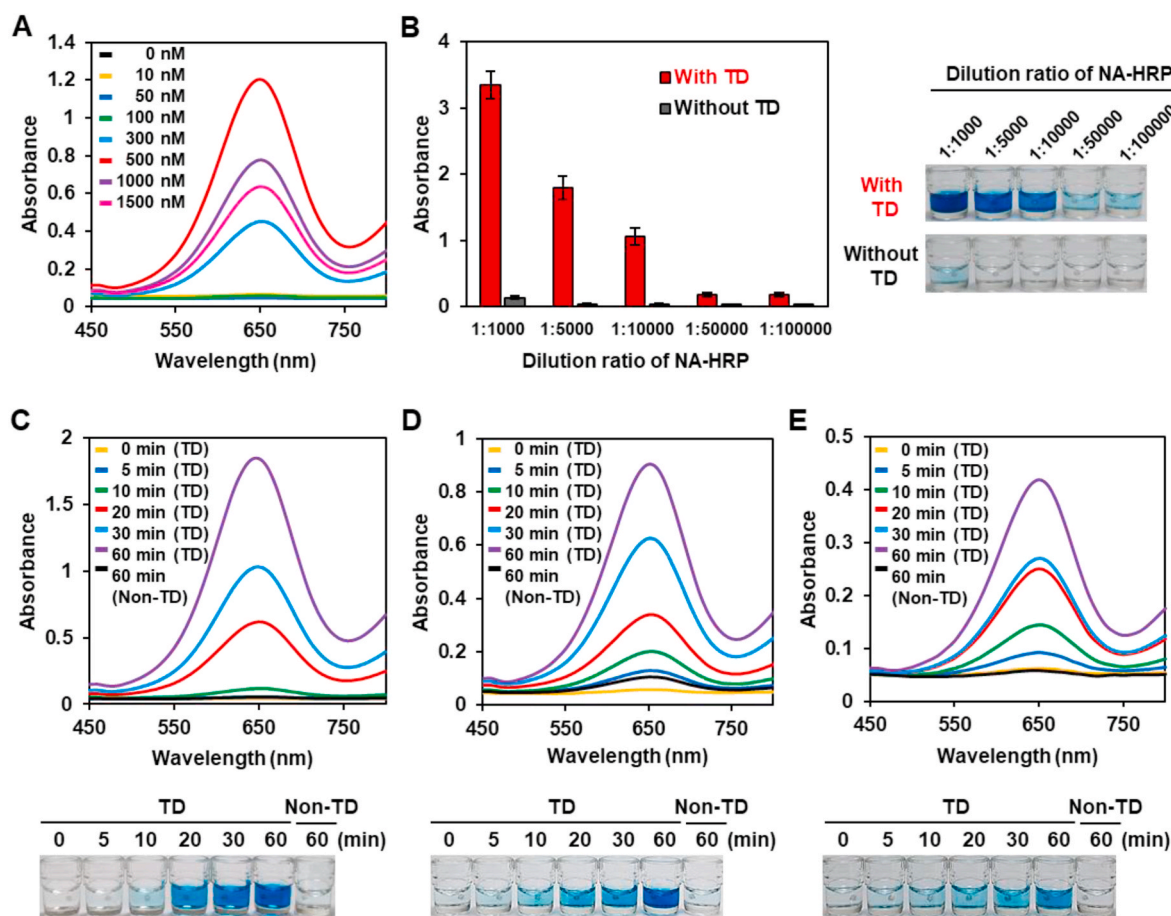


Fig. 2. (A) Absorbance spectra analysis to determine the optimized concentrations of HD for the CHA-based chemiluminescent assay. (B) Absorbance intensity (left panel) and corresponding photographs (right panel) to determine the optimized concentration of neutravidin-HRP by comparing the responsive color change in the presence and absence of target cDNA (TD). (C–E) Absorbance spectra analysis to determine (C) the adsorption time of dimeric DNA probes to the microplate wells, (D) the reaction time of neutravidin-HRP in the microplate wells with well-immobilized dimeric DNA probes, and (E) the color developing time of TMB solution. 500 nM of HDs was used to determine each optimized step. (For interpretation of the references to color in this figure legend, the reader is referred to the Web version of this article.)

Therefore, the dilution factor of neutravidin-HRP was selected at 1/5000 for a high detection sensitivity of the proposed CHA-based chemiluminescent assay.

We then examined the optimized time for each step of the CHA-based chemiluminescent assay for the rapid detection of target genes. The adsorption time of the biotinylated dimeric DNA probes onto the neutravidin-coated microplate wells was explored by adjusting their incubation time (Fig. 2C). The chemiluminescent signals showed a gradual increase as the adsorption time increased from 5 min to 60 min in the presence of TD. Notably, the corresponding color change from colorless to blue was detected at 10 min and turned completely dark blue after 20 min. However, in the absence of TD, no remarkable color change was observed for 60 min under the same conditions. This result indicates that the CHA-based chemiluminescent assay can precisely detect the target cDNA within 20 min at room temperature through colorimetric detection. The incubation time of NA-HRP in the dimeric DNA probe-loaded microplate wells was also investigated (Fig. 2D). Increasing the incubation times from 5 min to 60 min led to a gradual increase in the chemiluminescent signals, with the corresponding color change gradually turning from colorless to bright and ultimately dark blue. Thus, 10 min of incubation was chosen to be suitable for the interaction time between the NA-HRP and dimeric DNA probes in the microplate wells. Finally, we estimated the HRP/TMB reaction time for visible color development (Fig. 2E). Detectable chemiluminescent signals and colorless-to-blue color change were observed after 5 min of incubation. From this result, the color developing time adopted 5 min of incubation. Based on the findings, in sum, we selected 500 nM HD concentration, 20 min of adsorption time to immobilize the dimeric DNA probes in microplate wells, 10 min of reaction time for NA-HRP and dimeric DNA probe interaction, and 5 min of color developing time for the proposed CHA-based chemiluminescent assay.

3.4. Analytic performance of the CHA-based chemiluminescent assay

Under the optimized conditions, we evaluated the applicability of the developed CHA-based chemiluminescent assay for *N*-TD and *E*-TD. As shown in Fig. 3A, with increasing concentrations of *N*-TD from 0 nM to 500 nM, the chemiluminescent signals gradually increased, which indicated that the CHA-based chemiluminescent assay was highly dependent upon the concentration of the target cDNA. The corresponding color change also gradually turned bright and then deep dark blue with increasing TD concentrations. Furthermore, when compared to the obvious color change in the presence of *N*-TD, no significant color

change was observed in the absence of *N*-TD (0 nM) under the same conditions. Next, we determined the limit of detection (LOD) of the CHA-based chemiluminescent assay for the target cDNA (Fig. 3B). The absorbance intensity increased almost linearly at *N*-TD concentrations ranging from 0 nM to 31 nM. From linear regression analysis of the calibration curve, the LOD was estimated to be 1.05 nM based on three independent experiments. Notably, similar results of detection sensitivity for *E*-TD were also observed (Figure S1B). Thus, the proposed CHA-based chemiluminescent assay can be said to provide a simple, rapid, and excellent means for the colorimetric detection of short target genes. Furthermore, the proposed assay enables rapid detection, competitive with RT-PCR and ELISA systems (Table S2).

3.5. Specificity of the CHA-based chemiluminescent assay

To verify whether the proposed CHA-based chemiluminescent assay has high sequence-specificity in TD detection, we used various *N*-TD sequences including single-, two-, three-, multiple-, and all-base mismatches (SM *N*-TD, DM *N*-TD, TM *N*-TD, MM *N*-TD, and AM *N*-TD, respectively). As shown in Fig. 4, a significantly high level of absorbance intensity appeared only in the perfectly matched *N*-TD (0.174 ± 0.028 a.u.) compared to that of SM *N*-TD (0.072 ± 0.006 a.u.), DM *N*-TD (0.054 ± 0.004 a.u.), TM *N*-TD (0.054 ± 0.004 a.u.), MM *N*-TD (0.043 ± 0.004 a.u.), and AM *N*-TD (0.047 ± 0.004 a.u.). Moreover, the responsive color change from colorless to dark blue was detected only in *N*-TD, whereas no obvious color change was observed in SM *N*-TD, DM *N*-TD, TM *N*-TD, MM *N*-TD, or AM *N*-TD under the same conditions. These results indicate that the proposed CHA-based chemiluminescent assay can precisely detect TD sequences in complex biological samples.

4. Conclusion

In conclusion, we presented a highly simple, sensitive, and sequence-specific colorimetric detection approach for short single-stranded target cDNA relevant to SARS-CoV-2 RNA genes through the developed CHA-based chemiluminescent assay. By combining CHA with ELISA-mimicking techniques, target cDNA can be recycled to continuously produce dimeric DNA probes from two catalytic hairpin DNA assemblies containing biotin at the 5' ends. The resultant dimeric DNA probes were effectively immobilized in a neutravidin-coated microplate well and then captured neutravidin-HRP for color development, thus enabling the naked-eye detection of the target cDNA at room temperature. The proposed sensing system does not require expensive equipment, complex

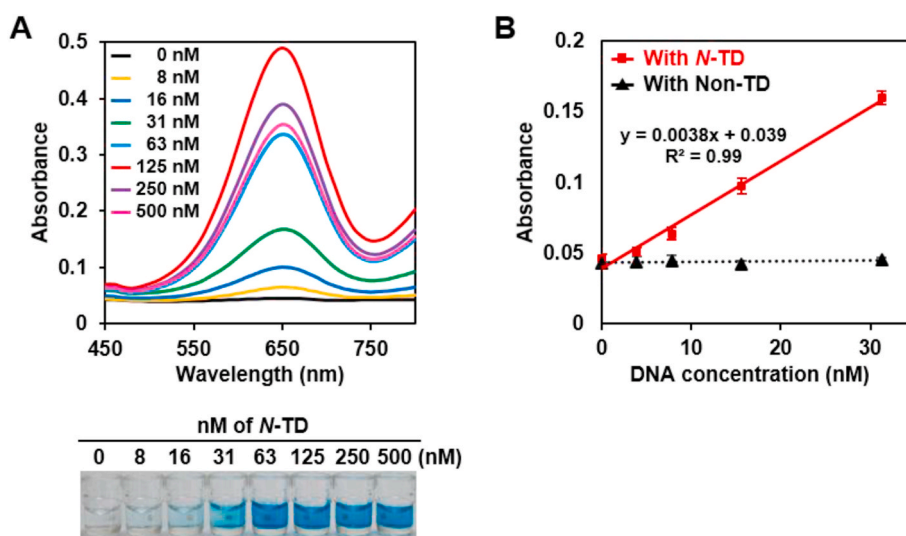


Fig. 3. (A) Absorbance spectra (upper panel) and corresponding photographs (lower panel) and (B) limit of detection (LOD) of the CHA-based chemiluminescent assay with increasing concentrations of *N*-TD under the optimized conditions. Error bars show the standard deviation of three independent experiments.

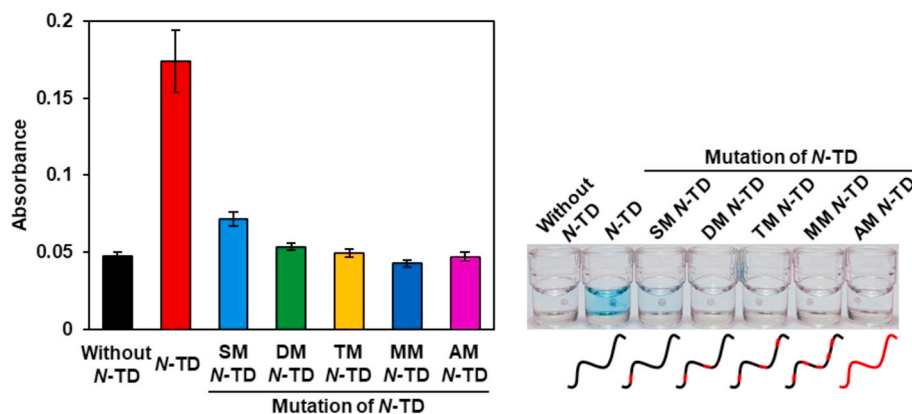


Fig. 4. Absorbance intensity (left panel) and corresponding photographs (right panel) of the CHA-based chemiluminescent assay in the presence of various *N* gene target cDNA (*N*-TD). The red sections of the *N*-TD strands corresponding to the above photograph indicate a mismatched single base toward target sequences. SM *N*-TD is a single-base mismatched target cDNA; DM *N*-TD is a two-base mismatched target cDNA; TM *N*-TD is a three-base mismatched target cDNA; MM *N*-TD is an *N*-TD multiple-base mismatched target cDNA; AM *N*-TD is an all-base mismatched target cDNA. Error bars show the standard deviation of three independent experiments. (For interpretation of the references to color in this figure legend, the reader is referred to the Web version of this article.)

protocols, or long time periods to amplify target DNA as compared to the typical requirements of enzyme-mediated DNA amplification. Therefore, we expect that the developed CHA-based chemiluminescent assay can be potentially utilized to detect a variety of short single-stranded target DNA as a colorimetric assay platform for biological diagnosis and pathological studies.

Declaration of competing interest

The authors declare that they have no known competing financial interests or personal relationships that could have appeared to influence the work reported in this paper.

Acknowledgements

This work was supported by a National Research Foundation of Korea (NRF) grant (NRF-2019R1G1A1099674) funded by the Korean government (Ministry of Science and ICT). This study was also supported by the Medi-Challenger Program funded by Gyeongsan City, and the Dongil Culture and Scholarship Foundation.

Appendix A. Supplementary data

Supplementary data to this article can be found online at <https://doi.org/10.1016/j.talanta.2021.122505>.

Authorship contribution statement

Ji Yoon Do: Conceptualization, Investigation, Methodology, Validation, and Writing-original draft preparation. **Ji Yun Jeong:** Conceptualization and Methodology. **Cheol Am Hong:** Supervision, Conceptualization, Methodology, Funding acquisition, and Writing-Reviewing and Editing.

References

- [1] E. Navarro, G. Serrano-Heras, M.J. Castaño, J. Solera, Real-time PCR detection chemistry, *Clin. Chim. Acta* 439 (2015) 231–250, <https://doi.org/10.1016/j.cca.2014.10.017>.
- [2] R.Y. Kim, H. Xu, S. Myllykangas, H. Ji, Genetic-based biomarkers and next-generation sequencing: the future of personalized care in colorectal cancer, *Per. Med.* 8 (2011) 331–345, <https://doi.org/10.2217/pme.11.16>.
- [3] L.L.M. Poon, C.S.W. Leung, M. Tashiro, K.H. Chan, B.W.Y. Wong, K.Y. Yuen, Y. Guan, J.S.M. Peiris, Rapid detection of the severe acute respiratory syndrome (SARS) Coronavirus by a loop-mediated isothermal amplification assay, *Clin. Chem.* 50 (2004) 1050–1052, <https://doi.org/10.1373/clinchem.2004.032011>.
- [4] L.L.M. Poon, K.H. Chan, O.K. Wong, W.C. Yam, K.Y. Yuen, Y. Guan, Y.M.D. Lo, J.S. M. Peiris, Early diagnosis of SARS Coronavirus infection by real time RT-PCR, *J. Clin. Virol.* 28 (2003) 233–238, <https://doi.org/10.1016/j.jcv.2003.08.004>.
- [5] A. Heim, C. Ebnet, G. Harste, P. Pring-Åkerblom, Rapid and quantitative detection of human adenovirus DNA by real-time PCR, *J. Med. Virol.* 70 (2003) 228–239, <https://doi.org/10.1002/jmv.10382>.
- [6] C. Jung, A.D. Ellington, Diagnostic applications of nucleic acid circuits, *Acc. Chem. Res.* 47 (2014) 1825–1835, <https://doi.org/10.1021/ar500059c>.
- [7] B. Li, A.D. Ellington, X. Chen, Rational, Modular adaptation of enzyme-free DNA circuits to multiple detection methods, *Nucleic Acids Res.* 39 (2011) e110, <https://doi.org/10.1093/nar/gkr504>.
- [8] Q. Li, Z. Liu, D. Zhou, J. Pan, C. Liu, J. Chen, A cascade toehold-mediated strand displacement strategy for label-free and sensitive non-enzymatic recycling amplification detection of the *HIV-1* gene, *Analyst* 144 (2019) 2173–2178, <https://doi.org/10.1039/c8an02340a>.
- [9] J. Liu, Y. Zhang, H. Xie, L. Zhao, L. Zheng, H. Ye, Applications of catalytic hairpin assembly reaction in biosensing, *Small* 15 (2019), 1902989, <https://doi.org/10.1002/smll.201902989>.
- [10] P. Yin, H.M.T. Choi, C.R. Calvert, N.A. Pierce, Programming biomolecular self-assembly pathways, *Nature* 451 (2008) 318–322, <https://doi.org/10.1038/nature06451>.
- [11] R.M. Dirks, N.A. Pierce, Triggered amplification by hybridization chain reaction, *Proc. Natl. Acad. Sci. Unit. States Am.* 101 (2004) 15275–15278, <https://doi.org/10.1073/pnas.0407024101>.
- [12] D. Yang, Y. Tang, P. Miao, Hybridization chain reaction directed DNA superstructures assembly for biosensing applications, *Trends Anal. Chem.* 94 (2017) 1–13, <https://doi.org/10.1016/j.trac.2017.06.011>.
- [13] H. He, J. Dai, G. Dong, H. Shi, F. Wang, Y. Qiu, R. Liao, C. Zhou, Y. Guo, D. Xiao, Self-replication-assisted rapid preparation of DNA nanowires at room temperature and its biosensing application, *Anal. Chem.* 91 (2019) 3043–3047, <https://doi.org/10.1021/acs.analchem.8b05431>.
- [14] S. Yue, X. Song, W. Song, S. Bi, An enzyme-free molecular catalytic device: dynamically self-assembled DNA dendrimers for *in situ* imaging of microRNAs in live cells, *Chem. Sci.* 10 (2019) 1651–1658, <https://doi.org/10.1039/c8sc04756a>.
- [15] H. Tan, X. Li, S. Liao, R. Yu, Z. Wu, Highly-sensitive liquid crystal biosensor based on DNA dendrimers-mediated optical reorientation, *Biosens. Bioelectron.* 62 (2014) 84–89, <https://doi.org/10.1016/j.bios.2014.06.029>.
- [16] S. Khajouei, H. Ravan, A. Ebrahimi, Developing a colorimetric nucleic acid-responsive DNA hydrogel using DNA proximity circuit and catalytic hairpin assembly, *Anal. Chim. Acta* 1137 (2020) 1–10, <https://doi.org/10.1016/j.aca.2020.08.059>.
- [17] Y. Liu, R. Liao, H. Wang, H. Gong, C. Chen, X. Chen, C. Cai, Accurate and sensitive fluorescence detection of DNA based on G-quadruplex hairpin DNA, *Talanta* 176 (2018) 422–427, <https://doi.org/10.1016/j.talanta.2017.08.003>.
- [18] Y. Liu, T. Shen, J. Li, H. Gong, C. Chen, X. Chen, C. Cai, Ratiometric fluorescence sensors for the microRNA determination by catalyzed hairpin assembly, *ACS Sens.* 2 (2017) 1430–1434, <https://doi.org/10.1021/acssens.7b00313>.
- [19] J. Zhu, Y. Ding, X. Liu, L. Wang, W. Jiang, Toehold-mediated strand displacement reaction triggered isothermal DNA amplification for highly sensitive and selective fluorescent detection of single-base mutation, *Biosens. Bioelectron.* 59 (2014) 276–281, <https://doi.org/10.1016/j.bios.2014.03.051>.
- [20] X. Liu, X. Zhou, X. Xia, H. Xiang, Catalytic hairpin assembly-based double-end DNAzyme cascade-feedback amplification for sensitive fluorescence detection of HIV-1 DNA, *Anal. Chim. Acta* 1096 (2020) 159–165, <https://doi.org/10.1016/j.aca.2019.10.051>.
- [21] J. Chen, J. Wen, L. Zhuang, S. Zhou, An enzyme-free catalytic DNA circuit for amplified detection of aflatoxin B1 using gold nanoparticles as colorimetric indicators, *Nanoscale* 8 (2016) 9791–9797, <https://doi.org/10.1039/c6nr01381c>.
- [22] C. Ma, W. Wang, Z. Li, L. Cao, Q. Wang, Simple colorimetric DNA detection based on hairpin assembly reaction and target-catalytic circuits for signal amplification, *Anal. Biochem.* 429 (2012) 99–102, <https://doi.org/10.1016/j.ab.2012.07.009>.
- [23] J. Wen, J. Chen, L. Zhuang, S. Zhou, SDR-ELISA: ultrasensitive and high-throughput nucleic acid detection based on antibody-like DNA nanostructure, *Biosens. Bioelectron.* 90 (2017) 481–486, <https://doi.org/10.1016/j.bios.2016.10.092>.
- [24] Q. Li, F. Zeng, N. Lyu, J. Liang, Highly sensitive and specific electrochemical biosensor for microRNA-21 detection by coupling catalytic hairpin assembly with rolling circle amplification, *Analyst* 143 (2018) 2304–2309, <https://doi.org/10.1039/c8an00437d>.

- [25] C. Zhong, G. Yang, N. Wang, F. Ji, Y. Zhang, X. Ding, J. Yang, J. Zhang, Hairpin assembly amplified electrochemical biosensor for highly sensitive and specific detection of DNA, *Electroanalysis* 28 (2016) 1578–1583. <https://doi.org/10.1002/elan.201501178>.
- [26] S. Liu, Y. Wang, J. Ming, Y. Lin, C. Cheng, F. Li, Enzyme-free and ultrasensitive electrochemical detection of nucleic acids by target catalyzed hairpin assembly followed with hybridization chain reaction, *Biosens. Bioelectron.* 49 (2013) 472–477. <https://doi.org/10.1016/j.bios.2013.05.037>.
- [27] L. Wu, G. Li, X. Xu, L. Zhu, R. Huang, X. Chen, Applications of nano-ELISA in food analysis: recent advances and challenges, *Trends Anal. Chem.* 113 (2019) 140–156. <https://doi.org/10.1016/j.trac.2019.02.002>.
- [28] C. Zhao, Y. Si, B. Pan, A.Y. Taha, T. Pan, G. Sun, Design and fabrication of a highly sensitive and naked-eye distinguishable colorimetric biosensor for chloramphenicol detection by using ELISA on nanofibrous membranes, *Talanta* 217 (2020), 121054. <https://doi.org/10.1016/j.talanta.2020.121054>.
- [29] M. Kimoto, Y.W.S. Lim, I. Hirao, Molecular affinity rulers: systematic evaluation of DNA aptamers for their applicabilities in ELISA, *Nucleic Acids Res.* 47 (2019) 8362–8374. <https://doi.org/10.1093/nar/gkz688>.
- [30] S. Guo, T. LakshmiPriya, S.C.B. Gopinath, P. Anbu, Y. Feng, Complementation of ELISA and an interdigitated electrode surface in gold nanoparticle functionalization for effective detection of human blood clotting defects, *Nanoscale Res. Lett.* 14 (2019) 222. <https://doi.org/10.1186/s11671-019-3058-z>.
- [31] T.G. Ksiazek, C.P. West, P.E. Rollin, P.B. Jahrling, C.J. Peters, ELISA for the detection of antibodies to Ebola viruses, *J. Infect. Dis.* 179 (1999) S192–S198. <https://doi.org/10.1086/514313>.
- [32] H.H. Garcia, L.J.S. Harrison, R.M.E. Parkhouse, T. Montenegro, S.M. Martinez, V.C. W. Tsang, R.H. Gilman, A specific antigen-detection ELISA for the diagnosis of human neurocysticercosis, *Trans. Roy. Soc. Trop. Med. Hyg.* 92 (1998) 411–414. [https://doi.org/10.1016/s0035-9203\(98\)91069-0](https://doi.org/10.1016/s0035-9203(98)91069-0).
- [33] S. Jäckel, M. Eiden, A. Balkema-Buschmann, M. Ziller, P. Jansen van Vuren, J. T. Paweska, M.H. Groschup, A novel indirect ELISA based on glycoprotein Gn for the detection of IgG antibodies against Rift Valley fever virus in small ruminants, *Res. Vet. Sci.* 95 (2013) 725–730. <https://doi.org/10.1016/j.rvsc.2013.04.015>.
- [34] J. Homsy, G.A. Thomson-Honniebier, C. Cheng-Mayer, J.A. Levy, Detection of human immunodeficiency virus (HIV) in serum and body fluids by sequential competition ELISA, *J. Virol Methods* 19 (1988) 43–56. [https://doi.org/10.1016/0166-0934\(88\)90006-7](https://doi.org/10.1016/0166-0934(88)90006-7).
- [35] L. Chen, F. Ruan, Y. Sun, H. Chen, M. Liu, J. Zhou, K. Qin, Establishment of sandwich ELISA for detecting the H7 subtype influenza A virus, *J. Med. Virol.* 91 (2019) 1168–1171. <https://doi.org/10.1002/jmv.25408>.
- [36] J.R. Wayment, J.M. Harris, Biotin-avidin binding kinetics measured by single-molecule imaging, *Anal. Chem.* 81 (2009) 336–342. <https://doi.org/10.1021/ac801818t>.
- [37] V.M. Corman, et al., Detection of 2019 novel coronavirus (2019-nCoV) by real-time RT-PCR, *Euro Surveill.* 25 (2020), 2000045. <https://doi.org/10.2807/1560-7917.ES.2020.25.3.2000045>.
- [38] R.K. Kakhki, M.K. Kakhki, A. Neshani, COVID-19 target: a specific target for novel coronavirus detection, *Gene Rep* 20 (2020), 100740. <https://doi.org/10.1016/j.genrep.2020.100740>.